International Journal of Marine Engineering Innovation and Research, Vol. 8(4), Dec. 2023. 598-604
(pISSN: 2541-5972, eISSN: 2548-1479)

Design and Performance Testing of a 3D Printed Mini DC Powered Pump for Microbubble Generator

Tulus H. Yusanto [1], James Julian[2], Fitri Wahyuni [3], Adi Winarta[4], I Wayan M. Managi [5]
(Received: 08 September 2023 / Revised: 08 September 2023 /Accepted: 18 September 2023)

***Abstract*—Centrifugal pumps are the most commonly utilized in industries, agriculture, and households. In the microbubble generator, the centrifugal pump is driven by a DC motor for efficiency. This research was conducted to determine the optimal centrifugal pump design for microbubble generators using 3D-printed PLA material. The pump drive uses a brushless DC motor. With impeller dimensions r_1=16mm, r_2=26mm, β_1=46.8, β_2=62.8, and number of blades = 8, the resulting head is 2m at a constant operational current of 3A and a flowrate of 0 L/m. The same operational current input yields a maximum flow rate of 14 L/min with a head of 0.5 m. Maximum head exists when there is no liquid on the outlet side. At current ≥ 6.5A, there is a deviation from the previously formed trend. The input power of 58W is generated when the maximum flow rate is 25L/m. Maximum efficiency can be achieved as the input current increases to ≤6.5A and 18L/m. At conditions ≥6.5A, efficiency decreases drastically as the input current increases. This centrifugal pump design can work optimally at a constant input current of 6.5A with an input power 58W for the microbubble generator.**

Keywords—Centrifugal pump, DC pump, 3d Printed, Efficiency, Flowrate, Head.

I. INTRODUCTION

The centrifugal pump is the most frequently utilized in industrial, agricultural, and household applications. Additionally, centrifugal pumps can be employed to create microbubble generator systems [1]–[4]. The microbubble pump is a device that generates air bubbles smaller than or equal to 50 micrometers in size and possesses various distinctive features resulting from its diminutive dimensions [5]. The microbubble pump can accurately generate microbubbles without the need for extra mechanical components. Microbubble pumps find applications in diverse sectors such as water treatment, biogas purification, green algae processing, fisheries, and healthcare. The generation of micro-sized gas bubbles by microbubble pumps results from the vigorous mixing of gas and liquid caused by the impeller's rotation within the pump. [6]–[8]. In order to achieve cost-effective pump design, it is essential to forecast its performance prior to the manufacturing phase, requiring a comprehension of flow characteristics within different pump elements. One approach for predicting performance is through experimental model testing, yet this method is laborious, unwieldy, and costly. Conversely, theoretical approaches only provide values but cannot identify the root causes of poor performance [9].

Nishi et al. have clarified that mini centrifugal pumps designed with traditional closed impellers outperform those utilizing semi-open impellers, according to conventional design methods. Nevertheless, it is deemed that semi-open impellers are more suitable for mini centrifugal pumps with regard to pump maintenance and impeller fabrication. Conversely, Nishi et al. have confirmed that commendable performance can be attained in semi-open impellers designed using innovative design techniques, featuring elevated blade outlet angles and increased blade numbers. [10]. Following this, a 55mm diameter semi-open impeller was selected for use in the mini centrifugal pump in this study, taking into account simplicity and ease of maintenance. Previous research had already revealed that the head of the mini centrifugal pump decreased due to viscosity effects. Furthermore, the study confirmed the positive impact of increasing the blade outlet angle on head improvement under conditions where rotation speed and pump size remained constant.

n the contrary, efficiency declined as the blade outlet angle increased due to intricate internal flow conditions [11], [12]. The objective of this study was to enhance the mini centrifugal pump's performance and internal flow characteristics, despite the inclusion of a significant blade outlet angle. Although the exact correlation between performance and flow conditions remained unclear, the research investigated the unpredictable performance and flow conditions of the mini centrifugal pump based on the results of numerical analysis. [13]. This study examined the size of bubbles and the concentration of microbubble pumps by controlling the inlet air flow rate and pump pressure at 4, 5, and 6 bars while keeping the impeller pump's rotation frequency constant. The findings indicated that a microbubble pump equipped with a

Tulus H. Yusanto, Departement of Mechanical Engineering, Universitas Pembangunan Nasional Veteran Jakarta, Jakarta, 12450, Indonesia. E-mail: tulus.hidayaty@upnvj.ac.id

James Julian, Departement of Mechanical Engineering, Universitas Pembangunan Nasional Veteran Jakarta, Jakarta, 12450, Indonesia. E-mail: zames@upnvj.ac.id

Fitri Wahyuni, Departement of Mechanical Engineering, Universitas Pembangunan Nasional Veteran Jakarta, Jakarta, 12450, Indonesia. E-mail: fitriwahyuni@upnvj.ac.id

Adi Winarta, Departement of Mechanical Engineering, Politeknik Negeri Bali, Badung, 80364, Indonesia. E-mail: adi.winarta@pnb.ac.id

I Wayan M. Managi, Departement of Mechanical Engineering, Politeknik Negeri Bali, Badung, 80364, Indonesia. E-mail: marlon_managi@pnb.ac.id

TABLE 1.
DESIGN PARAMETER OF IMPELLER

Impeller Specification	
Inlet Diameter	16mm
Outlet	26mm
β_1	46.8°
β_2	62.8°
Number of Blade	8

regenerative impeller generated a greater pressure differential from input to output and exhibited localized circulation flows on each blade. Among the three distinct pump pressures, the microbubble pump displayed its highest bubble concentration at a pressure of 5 bars, with the greatest concentration of bubbles falling within the diameter range of 20 to 30 micrometers. [14].

While research on microbubbles has been relatively limited thus far, this is particularly notable when considering factors such as bubble size and concentration generated by microbubble pumps under critical operational conditions for evaluating pump performance. This investigation delved into bubble size and concentration produced by the microbubble pump through experimental measurements. The characteristics of bubble particles were also evaluated by adjusting the inlet air flow rate and increasing pump pressure using a valve while maintaining a consistent impeller rotation frequency. All data were recorded and stored on a computer. The pump was designed in a miniaturized 3D format, smaller in scale compared to conventional pumps. In this study, the pump employed for the microbubble generation system underwent comprehensive experimental testing, analysis, and discussion.

II. METHOD

A. Construction of Pump

The pump used in this study is a single-stage centrifugal pump type with 3D-printed PLA material. The pump is 156 mm long, 100.76 mm wide, and 78.4 mm high. The pump sealing system in this study uses an o-ring between the shaft and the hole on the rear wall of the pump. The pump drive system uses a DC electric motor with specifications BLD C2435 Kv = 3300 rpm/volt waterproof. The construction of the pump and impeller is illustrated in Figure 1.

B. Construction of Impeller

The impeller used in this research centrifugal pump is of the semi-open eight-blade type with backward-facing vanes. This impeller features an inner diameter measuring 16 mm and an outer diameter of 26 mm, along with a blade thickness of 1.6 mm. The inlet angle β_1 on this impeller is 46.8°, and the outlet angle β_2 is 62.8°, see Table 1. The material used in this impeller is PLA 3D printed.

C. Construction of Impeller

The impeller used in this research centrifugal pump is of the semi-open eight-blade type with backward-facing vanes. This impeller has an inlet diameter of 16 mm and an outlet diameter of 26 mm with an impeller thickness of mm. The inlet angle β_1 on this impeller is 46.8°, and the outlet angle β_2 is 62.8°. The material used in this impeller is PLA 3D printed.

D. Mechanical Pump Theory

A centrifugal pump is one of the power-generating machines with varied applications and is used to convert rotational mechanical energy into fluid pressure energy [15]. When the pump is operating, the suction side of the pump has a pressure that is lower than atmospheric pressure. The fluid from the suction side will be sucked in and will enter the suction side of the pump so that fluid can move from one low point to a higher point. When moving fluid, the pump requires a certain amount of power to overcome friction losses in the pump and in the pipe itself [16], [17]. The impeller is a part of the pump that energizes the fluid by converting the mechanical energy of the blade rotation into pressure energy in the pumped fluid. When the blade rotates, a vacuum occurs on the suction side, which causes the fluid to be constantly sucked in to fill the vacuum space so the fluid will flow. There are three types of impeller. A closed impeller is the most common impeller used in many applications due to its high efficiency and head. Semi-open impeller feature lines that are open on one side and suitable for pumping a fluid with higher viscosity and more solid particles. The open impeller has the lowest efficiency and head but can work significantly under very high viscosity and solid particles in the fluid [18].

The rotational motion of the impeller leads to an elevation in pressure at the pump's outlet, resulting in an increase in its pump head. Centrifugal pump head denotes the energy dispensed by the pump to the fluid, enabling it to elevate the fluid to a designated height. The pump head is quantified in meters to assess the pump's efficacy in lifting the fluid to a predetermined elevation. Consequently, the specific head of the pump signifies the quantity of head generated by the pump. [19]. The formula for the pump-specific head can be seen in Equation 1.

$$H_p = \frac{P_2 - P_1}{\gamma} \tag{1}$$

The head of a pump also correlates with the pump's power. Power can be defined as the energy released by a

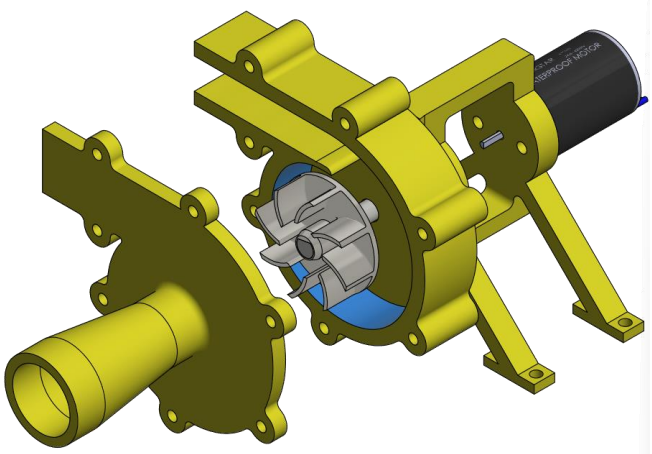

(a)

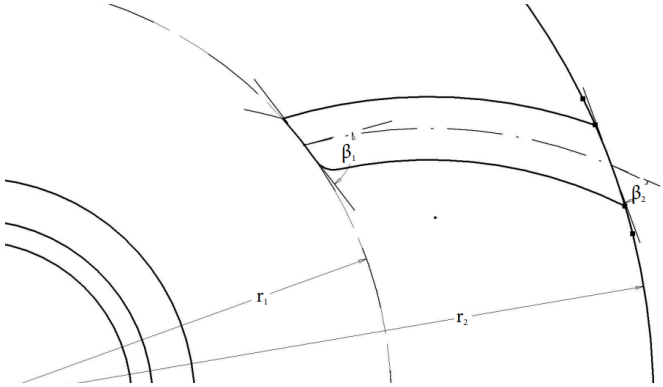

(b)

Figure 1.(a) isometric view of pump. (b) impeller contruction

power plant per unit time. Thus, the higher the pump head, the higher its power will be produced. The pump impeller supplies the pump's hydraulic power to the fluid to flow and is the product of the head, fluid flow, and fluid density. The hydraulic power of the pump is generally measured in joules per second or watts. The pump hydraulic power equation can be formulated in equation 2 [20].

$$P_{hydraulic} = \gamma \times Q \times H \quad (2)$$

The calculation of hydraulic power generation can also be applied to determine its efficiency. Pump efficiency can be described as the ratio between the output power generated by the pump and the input power supplied to the pump.. The output power of the pump can be called hydraulic power, while the input power can be called the driving power given to the pump shaft. So, pump efficiency can be written as the ratio between hydraulic and motor power driving the shaft [20]. The pump efficiency equation can be formulated in equation 3.

$$\eta_N = \frac{N_{hydraulic}}{N_{motor}} \quad (3)$$

III. RESULTS AND DISCUSSION

In this study, the pump, designed and manufactured using 3D printing, was experimentally tested on a test rig with the setup depicted in Figure 2 and Figure 3. The pump's input power was supplied using a DC power supply with maximum voltage and current outputs of 30V and 10A, respectively. Water at 20°C was used as the pump in the experiment. The controlled hydraulic variable was the water flow rate, while the controlled electrical variable was the inpu current (constant current). The supplied input current is varied with a range of variations starting from 3A, 5A, 6.5A, 7A, 8A, to 9A. Meanwhile, the input voltage is controlled by the power supply to produce the required current during pump operation. The constant current was used to prevent excessive current that could damage motor components and the driver while the pump operated.

The results of the conducted experiments show that the pump exhibits head characteristics, as presented in Figure 4. Under a current variation of 3A, the maximum head the pump can generate is 2m at a flow rate of 0 L/min and a maximum flow rate of 14 L/min with a head of 0.5m. Increasing the flow rate during constant current operation the pump also increase. This phenomenon is evident in the graphs for currents of 3A, 5A, and 6.5A. The increase in maximum head, typically occurring when no fluid exits

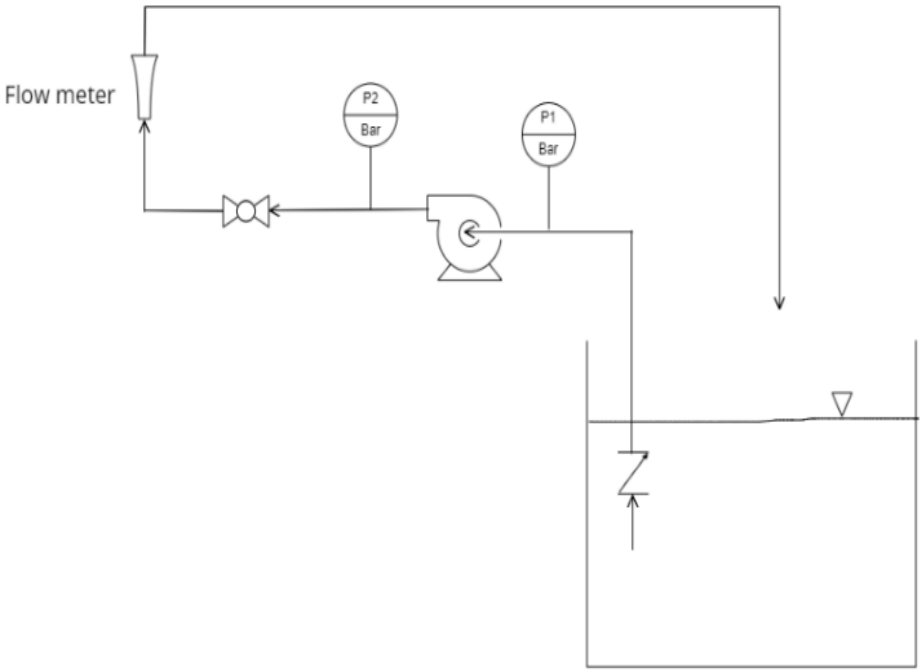

Figure 2. Efficiency of the pump at a constant current

Figure 3. Efficiency of the pump at a constant current

the outlet side (flow rate = 0 L/min), does not always apply due to the addition of input current. It can be inferred that there is a deviation from the previous trend for the head graph with currents ≥ 6.5A. At a flow rate of results in a reduction in head. As the input current increases, the maximum head and flow rate achievable by 0 L/min, the pump, operating at an input current of 7A, exhibits a head equal to that of the pump operating at 6.5A, which is 4.1m. However, at currents of 8A and 9A, the pump head experiences a significant decrease for unknown reasons. The highest head achieved by the pump is 4.1m at a flow rate of 18 L/min under an operational current of 9A.

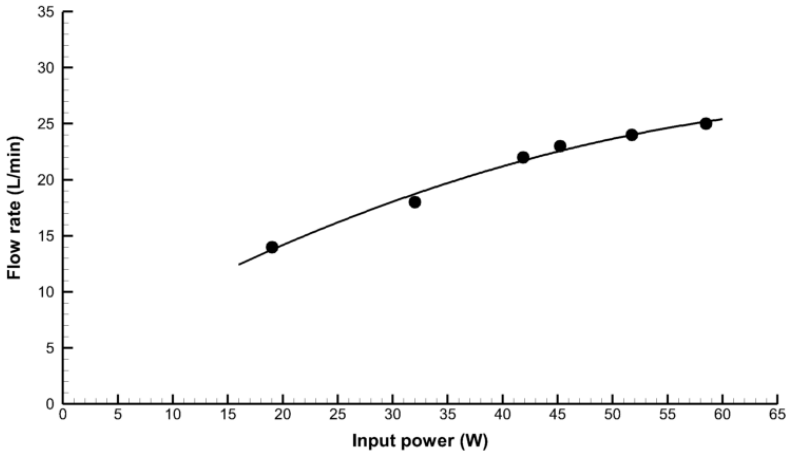
Flow rate (L/min)
Input power (W)

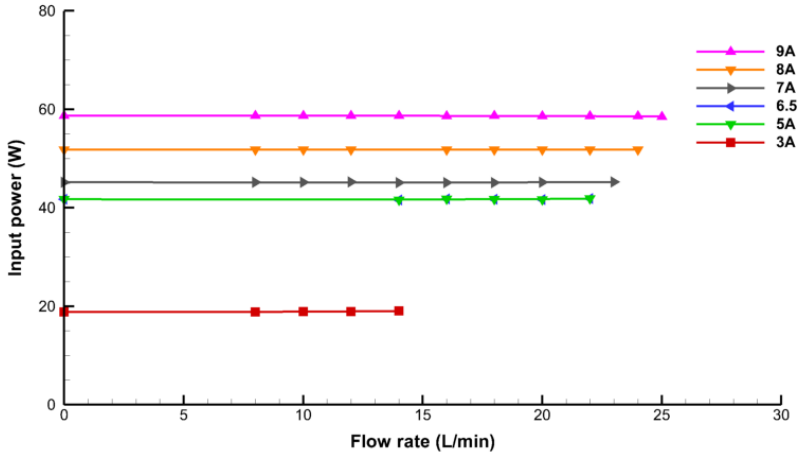
Input power (W)
Flow rate (L/min)
9A
8A
7A
6.5
5A
3A

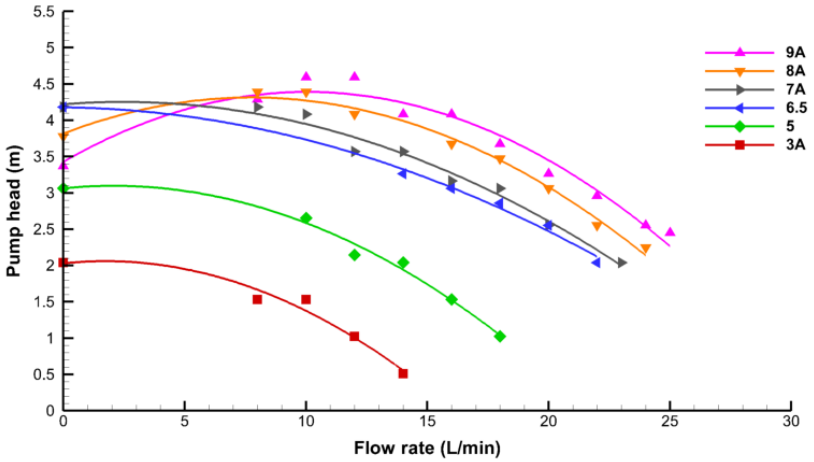
Pump head (m)
Flow rate (L/min)
9A
8A
7A
6.5
5
3A

Figure 5 illustrates the magnitude of input power supplied to the motor for various flow rate combinations and input current. Under constant current conditions, the power required by the motor is not significantly influenced by changes in flow rate. However, there is a limit to the flow rate that can be achieved for each operational current. This figure illustrates that under constant current operating conditions, the input power of the pump remains unaffected by any flowrate it produces. This aligns with the decrease in pump efficiency as the flowrate decreases, where the supplied input power remains constant, but the hydraulic power diminishes with the reduction in flowrate. The maximum flow rate that the pump can produce as a function of input power is shown in Figure 6. The flow rate generated by the pump increases with the increment of supplied power. In this study, the designed pump, with a relatively low input power of 58W, can generate a maximum flow rate of 25 L/min. When the input power supplied to the pump is 19W, the pump is capable to produce a maximum flow rate of 14 L/min. A flow rate of 18 L/min can be achieved by the pump with an input power of only 32W. At flow rates of 22, 23, and 24 L/min, the power required to drive the pump sequentially amounts to 42W, 45W, and 52W

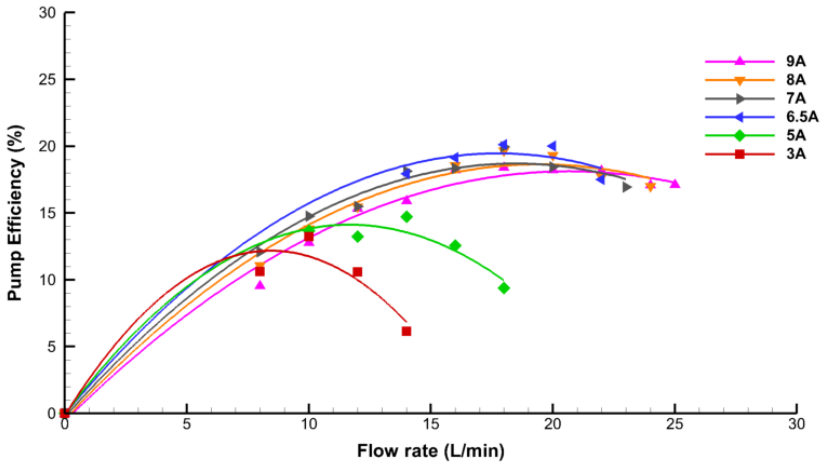

Figure 7. Efficiency of the pump at constant current

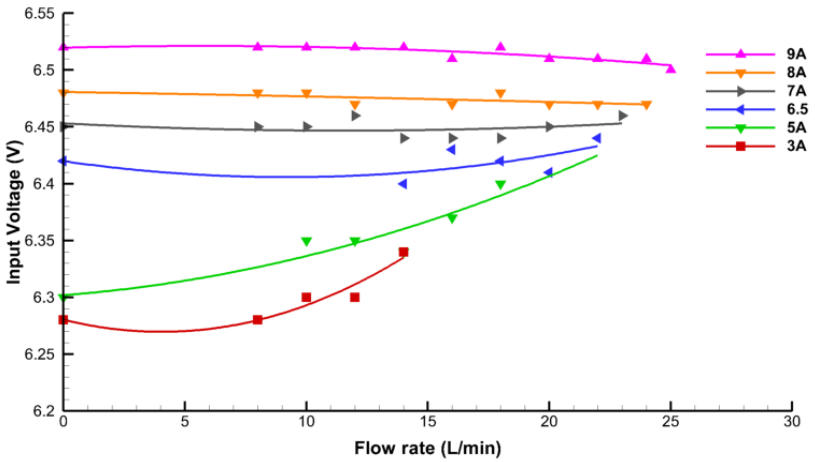

Figure 8. Input voltage of the pump

Concurrently with the head and flow rate it can produce, this pump exhibits efficiency characteristics, as shown in Figure 7. The pump's operational current and flow rate influence the magnitude of efficiency. Under low current conditions (<6.5A), the maximum efficiency that the pump can achieve increases as the input current rises. However, efficiency decreases with increasing input current at high currents (>6.5A). At an input current of 3A, the pump is capable of achieving its highest efficiency at 14%, while the efficiency at maximum flow rate (14 L/min) is 6%. Efficiency improvements occur as the pump's input current increases from 3A to 5A. At 5A input, the pump can reach its peak efficiency of 15% at a flow rate of 14 L/min. When the input current is further increased to 6.5A, the pump achieves its highest efficiency among all the test scenarios. The operational condition with a current of 6.5A at a flow rate of 18 L/min exhibits the highest efficiency at 20.1%. When the input current is increased again to 7A and 8A, the maximum efficiency that the pump can achieve remains unchanged

at 20% at a flow rate of 18 L/min. However, at an input current of 9A, the maximum efficiency attainable by the pump decreases to only 18% at 18 L/min.

Figure 8 depicts the magnitude of input voltage due to changes in flow rate at each constant current. This figure illustrates that, under constant input currents, input voltage increases with an increase in flow rate. This trend holds for input currents ≤6.5A, whereas for input currents >6.5A, input voltage decreases due to increased flow rate. At a constant input current of 3A, the maximum and minimum voltages supplied to the motor are 6.34V and 6.28V respectively. The voltage curve at an input current of 5A exhibits a trend that approaches linearity. The curve for the constant current of 9A shows that the input voltage supplied to the motor does not exceed 6.52V, and 6.35V for input currents of 3A. The pump with an input current of 7A exhibits a relatively constant input voltage of approximately 6.45V, regardless of the flowrate it produces. This may indicate a relatively constant shaft rotation, considering the DC motor's theoretical relationship between input voltage and rotational speed. Under operating conditions with 8A and 9A currents, the pump's voltage tends to decrease with increasing flowrate. This figure provides data on motor input voltage and current at each flowrate, which is valuable for determining the current and voltage capacity of the power supply to be used in the field for generating microbubbles. A microbubble generator requiring a head of 4 m can utilize this pump at a voltage of 6.52V with a power supply current capacity of ≥ 9A.

IV. CONCLUSION

The design of a centrifugal pump made using 3D printing has been carried out and tested experimentally. As a result, with manufacturing using 3D printing, efficiency values increase as the current increases to 20.1% at a flow rate of 18L/min with a constant operating current of 6.5A. However, the efficiency value will decrease when the operating current is >6.5A. With the same operational flow, the resulting head shows the best trend toward increasing the flow rate. However, when the applied current is more than 6.5A while the outlet is closed, the head is seen to drop to <3.5m. Meanwhile, the resulting maximum flow rate reaches 25L/minute with relatively small input power, namely 58W. Therefore, the pump design with 3D printing can operate optimally at a constant operating current of 6.5A with a maximum power of 58W for microbubble generator.

REFERENCES

[1] P. Usha and C. Syamsundar, "Computational analysis on performance of a centrifugal pump impeller," in *Proceedings of the 37th National & 4th International Conference on Fluid Mechanics and Fluid Power. Chennai, India, paper# TM-07*, 2010.

[2] Deendarlianto, Wiratni, A. E. Tontowi, Indarto, and A. G. W. Iriawan, "The implementation of a developed microbubble generator on the aerobic wastewater treatment," *International Journal of Technology*, vol. 6, no. 6, pp. 924–930, 2015, doi: 10.14716/ijtech.v6i6.1696.

[3] P. Li and H. Tsuge, "Water Treatment by Induced Air Flotation Using Microbubbles," *JOURNAL OF CHEMICAL ENGINEERING OF JAPAN*, vol. 39, no. 8, pp. 896–903, 2006, doi: 10.1252/jcej.39.896.

[4] X. Vilaida, S. Kythavone, and T. Iijima, "Effect of Throat Size on Performance of Microbubble Generator and Waste Water Treatment," *IOP Conf Ser Mater Sci Eng*, vol. 639, no. 1, p. 012031, 2019, doi: 10.1088/1757-899X/639/1/012031.

[5] S. Khuntia, S. K. Majumder, and P. Ghosh, "Microbubble-aided water and wastewater purification: a review," *Reviews in Chemical Engineering*, vol. 28, no. 4–6, pp. 191–221, 2012.

[6] S.-Y. Jeon, J.-Y. Yoon, and C.-M. Jang, "Optimal design of a novel 'S-shape'impeller blade for a microbubble pump," *Energies (Basel)*, vol. 12, no. 9, p. 1793, 2019.

[7] E. Tayama *et al.*, "Microbubble generation in roller and centrifugal pumps," *Journal of Artificial Organs*, vol. 2, pp. 58–61, 1999.

[8] R. C. da Silva Henauth, R. de Souza Vasconcelos, A. E. de Moura, L. A. Sarubbo, and V. A. dos Santos, "Microbubble generation with the aid of a centrifugal pump," *Chem Eng Technol*, vol. 40, no. 1, pp. 138–144, 2017.

[9] K. Patel and M. Satanee, "New development of high head Francis turbine at jyoti ltd. for small hydro power plant," *Proceedings of Himalayan Small Hydropower Summit. Dehradun, India, paper*, vol. 13, 2006.

[10] M. Nishi, "Tip-clearance effect on the performance of a high speed mini-turbopump," in *1998, Proceedings of The Third International Conference on Pumps and Fans Beijing, China*, 1998, pp. 223–231.

[11] T. Shigemitsu, J. Fukutomi, R. Nasada, and K. Kaji, "The effect of blade outlet angle on performance and internal flow condition of mini turbo-pump," *Journal of Thermal Science*, vol. 20, pp. 32–38, 2011.

[12] E. C. Bacharoudis, A. E. Filios, M. D. Mentzos, and D. P. Margaris, "Parametric study of a centrifugal pump impeller by varying the outlet blade angle," *The Open Mechanical Engineering Journal*, vol. 2, no. 1, 2008.

[13] T. Shigemitsu, J. Fukutomi, K. Kaji, and T. Wada, "Performance and internal flow condition of mini centrifugal pump with splitter blades," *International Journal of Fluid Machinery and Systems*, vol. 6, no. 1, pp. 11–17, 2013.

[14] S.-Y. Jeon, J.-Y. Yoon, and C.-M. Jang, "Bubble size and bubble concentration of a microbubble pump with respect to operating conditions," *Energies (Basel)*, vol. 11, no. 7, p. 1864, 2018.

[15] H. Wang, B. Long, C. Wang, C. Han, and L. Li, "Effects of the impeller blade with a slot structure on the centrifugal pump performance," *Energies (Basel)*, vol. 13, no. 7, p. 1628, 2020.

[16] X. Han, Y. Kang, D. Li, and W. Zhao, "Impeller optimized design of the centrifugal pump: A numerical and experimental investigation," *Energies (Basel)*, vol. 11, no. 6, p. 1444, 2018.

[17] J. H. Kim, K. T. Oh, K. B. Pyun, C. K. Kim, Y. S. Choi, and J. Y. Yoon, "Design optimization of a centrifugal pump impeller and volute using computational fluid dynamics," in *IOP Conference Series: Earth and Environmental Science*, IOP Publishing, 2012, p. 032025.

[18] H. Bozorgasareh, J. Khalesi, M. Jafari, and H. O. Gazori, "Performance improvement of mixed-flow centrifugal pumps with new impeller shrouds: Numerical and experimental investigations," *Renew Energy*, vol. 163, pp. 635–648, 2021.

[19] A. J. Acosta and R. D. Bowerman, "An Experimental Study of Centrifugal-Pump Impellers," *Transactions of the American Society of Mechanical Engineers*, vol. 79, no. 8, pp. 1821–1839, Feb. 2022, doi: 10.1115/1.4013503.

[20] R. Barmaki and M. B. Ehghaghi, "Experimental investigation of a centrifugal pump hydraulic performance in hydraulic transmission of solids," *Mechanics and Mechanical Engineering*, vol. 23, no. 1, pp. 259–270, 2019, doi: 10.2478/mme-2019-0035.